

Synergistic Feature Fusion for Accurate Skin Cancer Classification

THIRUMALADEVI S¹, VEERASWAMY K², M SAILAJA³, SADULLA SHAIK⁴

^{1,4}Department of Electronics and Communication Engineering, KKR & KSR Institute of Technology and Sciences, Vinjanampadu-522017, Guntur, Andhra Pradesh, India Pradesh, India.

²Department of Electronics and Communication Engineering, Vasavi College of Engineering, Ibrahimbagh, Hyderabad - 500 031, Telangana, India.

³Department of Electronics and Communication Engineering, Jawaharlal Nehru Technological University, Kakinada-533003, Andhra Pradesh, India.

Email: thirumaladevice@gmail.com¹, k.veeraswamy@staff.vce.ac.in², sailaja.maruvada@gmail.com³, sadulla09@gmail.com⁴

Received: 11.09.23, Revised: 21.10.23, Accepted: 18.11.23

ABSTRACT

Skin cancer is considered one of the most dangerous types of cancer caused by damaged DNA, and it can be life-threatening. The abnormal DNA leads to uncontrolled cell growth, and the cancer can spread rapidly. Analyzing skin lesion images for cancer detection is challenging due to various factors such as light reflections, color variations, difficulty in identification and diagnosis, varying sizes and shapes of lesions, and the similarity between different skin diseases like melanoma and nevus. Automatic recognition of skin cancer can be beneficial in improving the accuracy and efficiency of pathologists in early detection. The proposed approach involves several steps to enhance the classification accuracy. First, the input images are normalized to account for variations in lighting and other factors. Then, features are extracted from the normalized images to aid in precise classification. Finally, feature fusion techniques are employed to improve the overall classification accuracy. In this investigation, models such as AlexNet, VGG-19, and VGG-16 were utilized. Compared to existing models, the results of the suggested model indicate higher reliability and robustness. By employing normalization, feature extraction, and feature fusion techniques, the proposed model aims to provide accurate and trustworthy skin cancer classification. To evaluate the performance of the proposed concept the Skin Cancer International Skin Imaging Collaboration's (ISIC) dataset was used to test the model, and a testing accuracy of 86.8% was achieved. This can contribute to the early detection of skin cancer, ultimately improving patient outcomes and assisting pathologists in their diagnostic process.

Keywords: AlexNet, Convolutional neural network, Feature fusion Classification, Pre-processing, Skin cancer, VGG-16 and VGG-19.

1. INTRODUCTION

Cancer is an imminent threat to human life. It may occasionally result in human death. There are various varieties of cancer that can occur in the human body, and skin cancer is one of the most rapidly developing diseases that can be fatal. Smoking, drinking, infections, allergies, viruses, exercise, environmental changes, and being exposed to ultraviolet (UV) light are just a few of the causes. Sunlight's UV rays have the potential to damage skin cells' DNA [1]. Skin cancer can indeed be associated with unusual swellings or growths on the skin. The four most common types of skin cancer are actinic keratoses, basal cell carcinoma, squamous cell carcinoma, and melanoma. It is important to monitor any unusual swellings or changes in the skin and consult a healthcare professional if you notice any concerning signs. Early intervention

plays key roles in the prevention and management of skin cancer.

Skin cancer is one of every three malignancies identified, based on the World Health Organisation (WHO) [2]. Over the last few decades, the number of persons diagnosed with skin cancer has progressively increased in the United States, Canada, and Australia. Each year, it is anticipated that 5.4 million instances of skin cancer will get diagnosed in the United States. The demand for quick and accurate clinical testing is increasing by the day [3]. Malignant melanoma is a type of cancer that arises from melanocytes in the epidermis of the skin. This form of cancer may have spread rapidly making treatment more challenging. As a result, early skin cancer detection may lead to treatment and identification, potentially saving lives. In recent decades, different kinds of computer-aided

diagnosis (CAD) systems have been proposed to diagnose skin cancer[4]. Traditional computer vision techniques are usually used as a classifier to extract many different properties such as form, size, colour, and texture to diagnose cancer. Artificial intelligence (AI) is now able to dealing with these difficulties. Deep neural networks (DNN), convolutional neural networks (CNN), long short term memory (LSTM), and recurrent neural networks (RNN) are the most extensively utilized deep-learning architectures in the medical industry for detecting cancer cells [5]. These models are also effective in classifying skin cancer. Furthermore, CNN, which is a DNN, has already produced tremendous results in this field. CNN is the most popular model, which is a collection of machine learning algorithms used for feature learning, and it is employed in these disciplines in huge data sets to increase the accuracy of the results. Melanoma is a form of skin cancer that causes malignant tumours on the skin. Dermatologic images are used to detect skin cancer [6]. Machine learning based on high-performance images is utilized to identify skin cancer, with good identification efficiency. CNN was used to detect skin cancer in dermoscopic images from pigmented melanocytic lesions. However, screening for non-melanocytic and non-pigmented skin cancer was problematic. It also had a reduced detection accuracy. The challenges of skin cancer are recognised and might be discussed below after reading the literature and watching various techniques. Challenges of skin cancer detection: Some challenges in detecting skin cancer can be attributable to differences in image kinds and sources. Human skin colour diversity makes skin cancer detection more difficult and complex.

- The main obstacles in skin cancer are the various sizes and shapes of the images, which make reliable identification impossible.

- Low contrast from neighbouring tissues can also add to the difficulty of analysing skin cancer correctly.
- Colour illumination presents additional challenges due to characteristics such as colour texture, light beams, and reflections.

The remainder of this work is divided into four sections. Section 1 Introduction, Section 2 provides a quick overview of feature extraction, therecommended technique for Fusion approach, Section 3 presents a description of the tests carried out and the results achieved. Section 4 contains the conclusion.

2. RELATED WORK

Feature extraction is a technique used in image processing to organise images into more manageable groups for subsequent processing [7]. In this investigation, we extract a considerable number of attributes from a wide number of datasets that aid in pattern detection and recognition [8]. Furthermore, it grabs and combines variables to extract characteristics that reduce the number of resources while preserving raw data information.

All pre-trained CNNs require fixed-size input images. Defining the desired image size and building augmented image data stores that are utilized as input arguments to activations are required [9]. FC layer FC8 should be removed from the pre-trained CNN and used as a static feature extractor. We feed a scene image into the CNN and, ahead of time, generate a dimensional activation vector from the first or second FC layer to serve as a representation of the input image's global features. Finally, to categorize scenes, a linear classifier should be trained using the dimensional properties. Figure 1 shows one representation of this.

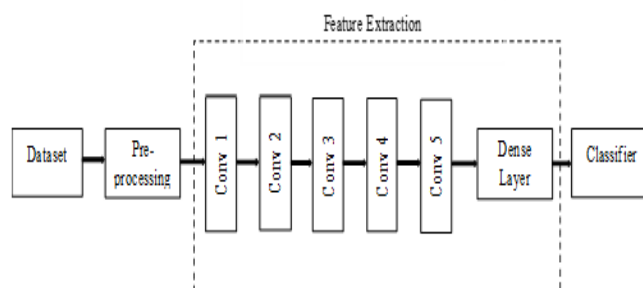


Figure 1: Representation of pre-trained CNN was used as a feature extractor

2.1 Multi-Layer Fusion

To improve classification accuracy, a modified pre-trained network design with input from

several convolution layers. The lower-level visual components, The shallower levels of the CNN model are more likely to represent edges, whilst

the deeper layers represent the more abstract data included in the images[10].

The method we suggest uses a similar process to benefit from the knowledge retained by multiple layers in this manner. Figure 2 depicts this in a visual manner. Here the features produced from the last three blocks of pre-trained networks' convolutional layers are concatenated. These would be conv3, conv4, and conv5, in the case of alexnet, and "conv3-3," "conv4-3," and "conv5-3," in the case of

vgg16 and vgg19, respectively. Because the multiple convolutional layers have distinct spatial dimensions, they cannot be concatenated directly. Down sampling with bilinear interpolation and channel-wise average fusion are used in tandem to overcome this problem. The collected characteristics were then reorganized into a matrix along the channel dimension before being aggregated with the help of covariance.

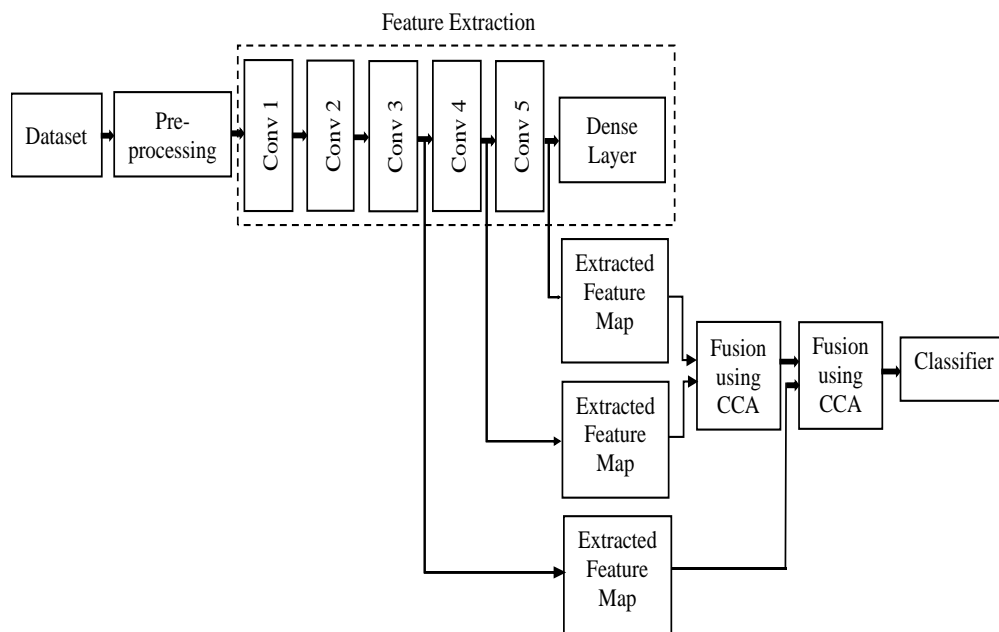


Figure 2: Multilayer fused pretrained CNN representation.

2.2 Canonical Correlation Analysis

Canonical correlation analysis (CCA) is a statistical technique that describes the relationship between the original and subsequent second sets of data. To put it another way, it's a method for deducing facts from matrices of cross-covariance.

It is becoming increasingly difficult to successfully blend multiple features[11]. Using the canonical correlation method, herecombine two independent feature vectors to create a new feature vector with an improved discriminative feature. When this method is applied to the correlation analysis of two random vectors, it produces various sets of uncorrelated pairsof variables. M and N vector matrices have zero mean values and are hence deemed arbitrary. Determine a couple of the orientations that will increase the correlation of the projection. Choose some common variables to utilise. Two features matrices M and N, in addition, $M \in R^{an}$ and $N \in R^{bn}$ where n is the training feature vectors containing the matrices. M's covariance

matrix is epitomized as $C_{pp} \in R^{axa}$ as well as $C_{qq} \in R^{bxb}$ is the covariance matrix of Nbetween sets the Covariance matrix is $C_{pq} \in R^{axb}$ and $C_{qp} = C_{pq}^T$ Overall covariance matrix

$C \in R^{(a+b) \times (a+b)}$ is deliberate as $C = \begin{pmatrix} cov(p) & cov(p,q) \\ cov(q,p) & cov(q) \end{pmatrix} = \begin{pmatrix} C_{pp} & C_{pq} \\ C_{qp} & C_{qq} \end{pmatrix}$ (1)

Because the correlations between two sets of feature vectors may not follow a predictable pattern, deducing the correlations between all of these matrices and two pairs of feature vectors may be difficult. The goal of correlation minimization linear combination analysis (CCA) [12] is to describe such an approach.

$M^* = W_p^T M$ and $N^* = W_q^T N$ (2)
 $Corr(M^*,N^*) = \frac{cov(M^*,N^*)}{var(M^*) \cdot var(N^*)}$ (3)

Wherever $var(M^*) = W_p^T C_{pp} W_p$
 $var(N^*) = W_q^T C_{qq} W_q$
 $cov(M^*, N^*) = W_p^T C_{pq} W_q$

Exploiting the covariance between M^* and N^* considering the constraints $\text{var}(M^*) = \text{var}(N^*) = 1$. The transformation matrices W_p, C_{pq}, W_q is initiated by especially the eigenvalue concerns.

$$\begin{cases} C_{pp}^{-1} C_{pq} C_{yy}^{-1} C_{qp} \widehat{W}_x = R^2 \widehat{W}_p \\ C_{qq}^{-1} C_{qp} C_{pp}^{-1} C_{pq} \widehat{W}_y = R^2 \widehat{W}_q \end{cases} \quad (4)$$

Where \widehat{W}_p and \widehat{W}_q are eigenvectors. R^2 is A diagonal matrix with the greatest eigenvalues or correlation squares. This is the number of eigenvalues that are not zero in each equation: $d = \text{rank}(C_{pq}) \leq \min(n, a, b)$ which is to be listed in descending manner

- $\alpha_1 \geq \alpha_2 \geq \alpha_3 \dots \geq \alpha_d$.
- $\alpha_1^T M$ and $\beta_1^T N$ (the first pair)
 - $\alpha_2^T M$ and $\beta_2^T N$ (the second pair)
 - $\alpha_d^T M$ and $\beta_d^T N$ (the dth pair)

$$\begin{aligned} M^* &= (\alpha_1^T M, \alpha_2^T M, \dots, \alpha_d^T M) = \\ (\alpha_1, \alpha_2, \dots, \alpha_d)^T M &= W_p^T \quad (5) \\ N^* &= (\beta_1^T N, \beta_2^T N, \dots, \beta_d^T N) \\ &= (\beta_1, \beta_2, \dots, \beta_d)^T N = W_q^T \end{aligned}$$

The organised eigenvectors that are equivalent to non-zero eigenvalues are used to generate the transformation matrices W_p and W_q .

$$C^* = \begin{pmatrix} 1 & 0 & \dots & 0 & r_1 & 0 & \dots & 0 \\ 0 & 1 & \dots & 0 & 0 & r_2 & \dots & 0 \\ \vdots & & \ddots & & & & \ddots & \\ 0 & 0 & \dots & 1 & 0 & 0 & \dots & r_d \\ - & - & - & - & - & - & - & - \\ r_1 & 0 & \dots & 0 & 1 & 0 & \dots & 0 \\ 0 & r_2 & \dots & 0 & 0 & 1 & \dots & 0 \\ \vdots & & \ddots & & \vdots & & \ddots & \\ 0 & 0 & \dots & r_d & 0 & 0 & \dots & 1 \end{pmatrix}$$

To do feature-level fusion, a sum of the adjusted extracted features is employed. Canonical discriminant correlation Included are the following features

$$\begin{aligned} Z_1 &= \begin{pmatrix} M^* \\ N^* \end{pmatrix} = \begin{pmatrix} W_p^T P \\ W_q^T Q \end{pmatrix} = \begin{pmatrix} W_p & 0 \\ 0 & W_q \end{pmatrix}^T \begin{pmatrix} P \\ Q \end{pmatrix} \quad (6) \\ Z &= M^* + N^* = (W_p^T M + W_q^T N) \\ &= \begin{pmatrix} W_p \\ W_q \end{pmatrix}^T \begin{pmatrix} M \\ N \end{pmatrix} \quad (7) \end{aligned}$$

CCA benefits are easily transferred between two variables. According to CCA, modalities have a linear relationship and can be viewed as counterparts with the same weight [10]. Linear feature adjustments have no effect on canonical correlations.

3. EXPERIMENTAL RESULTS DISCUSSION

The skin cancer images used for feature extraction are scaled to the specifications of the input layer, which is 227x227x3 for Alex Net and 224x224x3 for VGG-16 and 19. ImageNet has been used to train both of these models. The Skin Cancer ISIC data set is utilized to train 80% of the samples and test 20%. The most commonly used quality measures for classification evaluation are the OA and confusion matrices, as well as Precision, Recall, and the F1-score. A positive sample anticipated to be positive (TP), and a positive sample predicted to be negative (FN). TN, like FP, denotes the number of negative events that were expected to be positive represents the number of negative occurrences that have occurred. The fraction of correct occurrences is known as accuracy, and the formula for calculating

$$\text{Overall Accuracy} = \frac{TP}{TP+FN+TN+FP} \quad (5.1)$$

Precision is defined as the proportion of real positives among all cases projected to be positive. The formula is as follows:

$$\text{Precision} = \frac{TP}{TP+FP} \quad (5.2)$$

Recall The calculation equation is the fraction of expected positive samples among all positive samples.

$$\text{True Positive Rate (or) Recall} = \frac{TP}{TP+FN} \quad (5.3)$$

A statistic for evaluating a test's accuracy is the F1 score. The test's precision and recall are used to calculate the harmonic mean of its recall and accuracy.

$$F1 = \frac{2 \times \text{Precision} \times \text{Recall}}{\text{Precision} + \text{Recall}} \quad (5.4)$$

Skin Cancer ISIC Dataset

The International Skin Imaging Collaboration's (ISIC) collection of images includes both malignant and benign oncological disorders. With the notable exception of melanomas and moles, whose images show a slight predominance, all subsets were divided into the equal number of images and all images were categorised according to the ISIC category. Actinic keratosis, basal cell carcinoma, dermatofibroma, melanoma, nevus, pigmented benign keratosis, seborrheic keratosis, squamous cell carcinoma, and vascular lesion are all included in the data set. Figure 3 exhibits visual examples for each kind.

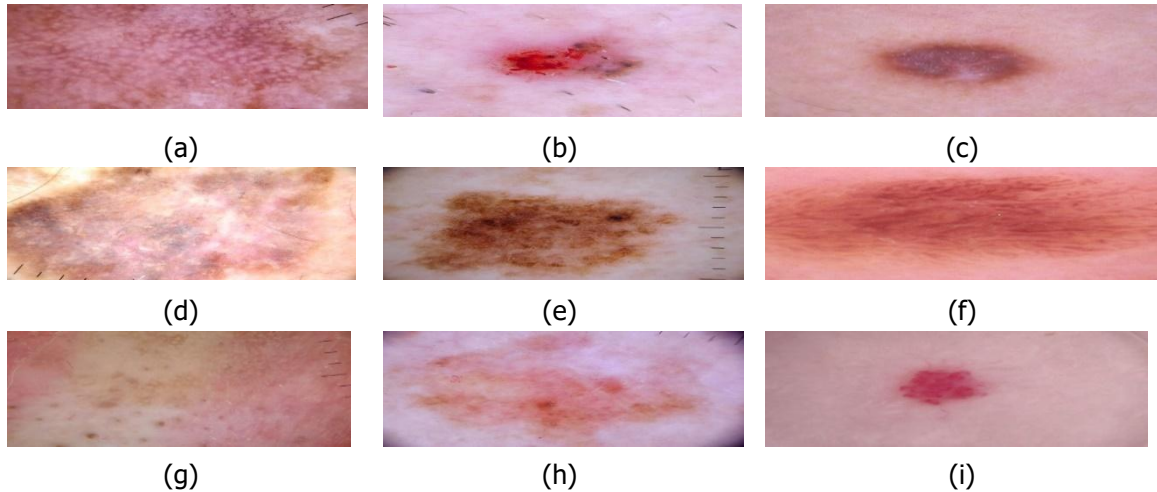
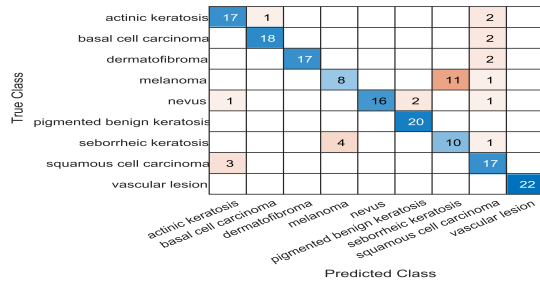
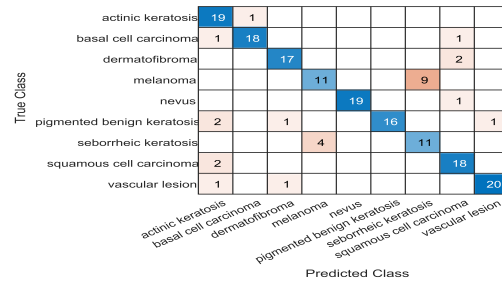


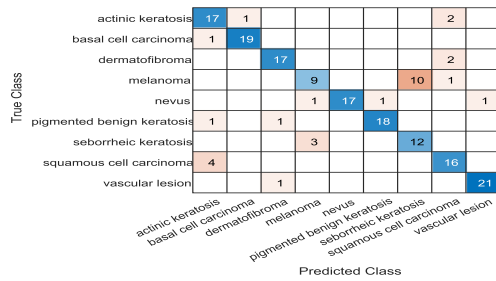
Figure 3: Skin Cancer ISIC Dataset (a) actinic keratosis3, (b) basal cell carcinoma7, (c) dermatofibroma9, (d) melanoma12, (e) nevus17, (f) pigmented benign keratosis5 (g) seborrheic keratosis6, (h) squamous cell carcinoma8 and (i) vascular lesion2.



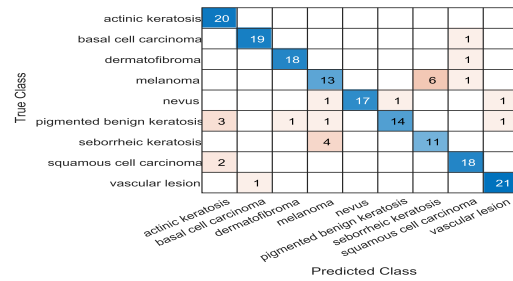
(a) 82.4



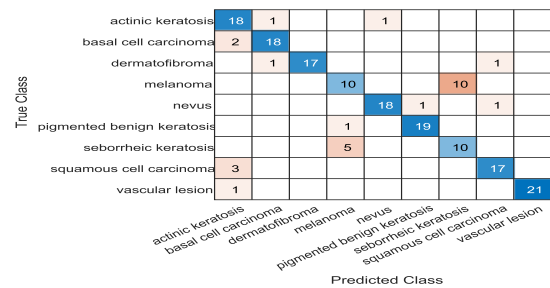
(b) 84.7



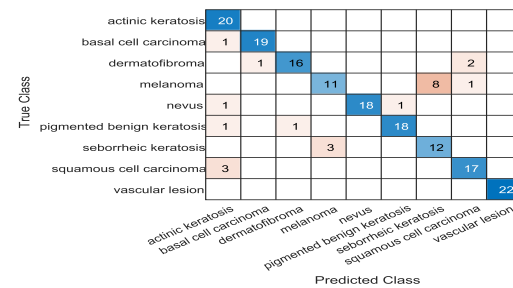
(c) 83



(d) 85.8



(e) 84.1



(f) 86.9

Figure 4: Confusion matrices of pre- trained and proposed networks (a) Alex Net (b)Proposed Alex Net (c)VGG 19 (d)Proposed VGG 19 (e) VGG 16 (f) Proposed VGG 16

Table 1: Metrics calculated for Alex Net and Proposed Alex Net

Class/ Parameter	Alex Net			Proposed Alex Net		
	Precision	Recall	F1 Score	Precision	Recall	F1 Score
actinic keratosis	85	81	82.95	95	76	84.44
basal cell carcinoma	90	94.7	92.29	90	94.7	92.29
dermatofibroma	89.5	100	94.46	89.5	89.5	89.5
melanoma	40	66.7	50.01	55	73.3	62.84
nevus	80	100	88.89	95	100	97.44
pigmented benign keratosis	100	90.9	95.23	80	100	88.89
keratosis	66.7	47.6	55.55	73.3	65	68.9
squamous cell carcinoma	85	65.4	73.92	90	81.8	85.7
vascular lesion	100	100	100	90.9	95.2	93

Table 2: Metrics calculated for VGG 19 and Proposed VGG 19

Class/ Parameter	VGG 19			Proposed VGG 19		
	Precision	Recall	F1 Score	Precision	Recall	F1 Score
actinic keratosis	85	73.9	79.06	100	80	88.89
basal cell carcinoma	95	95	95	95	95	95
dermatofibroma	89.5	89.5	89.5	94.7	94.7	94.7
melanoma	45	69.2	54.54	65	68.4	66.66
nevus	85	100	91.89	85	100	91.89
pigmented benign keratosis	90	94.7	92.29	70	93.3	79.99
keratosis	80	64.5	71.42	73.3	64.7	68.73
squamous cell carcinoma	80	76.2	78.05	90	85.7	87.8
vascular lesion	95.5	95.5	95.5	95.5	91.3	93.35

Table 3: Metrics calculated for VGG 16 and Proposed VGG 16

Class/ Parameter	VGG 16			Proposed VGG 16		
	Precision	Recall	F1 Score	Precision	Recall	F1 Score
actinic keratosis	90	75	81.82	100	76.9	86.94
basal cell carcinoma	90	90	90	95	95	95
dermatofibroma	89.5	100	94.46	84.2	94.1	88.88
melanoma	50	62.5	55.56	55	78.6	64.72
nevus	90	94.7	92.29	90	100	94.74
pigmented benign keratosis	95	95	95	90	94.7	92.29
keratosis	66.7	60	63.17	80	60	68.57
squamous cell carcinoma	85	89.5	87.19	85	85	85
vascular lesion	95.5	100	97.7	100	100	100

The Figure 4 represents the overall accuracy confusion matrices for all three existing and proposed networks. The categorization accuracy of proposed networks is tabulated and it is visually compared. Table 1 represents the metrics comparison of Alex Net, Proposed Alex Net. Table 2 represents the metrics comparison of VGG 19, Proposed VGG 19. Table 3 represents the metrics comparison of VGG 16, Proposed VGG 16. Figure 5 represents the F1 scores of Alex

Net and Proposed Alex Net. Out of Nine classes five classes improves their F1 score actinic keratosis, melanoma, nevus, keratosis, squamous cell carcinoma. Remaining are dematofibroma, pigmented benign keratosis, vascular lesion. Figure 6 represents the F1 scores of VGG 19 and Proposed VGG 19. Out of Nine classes five classes improves their F1 score actinic keratosis, dermatofibromamelanoma, nevus, squamous cell carcinoma.

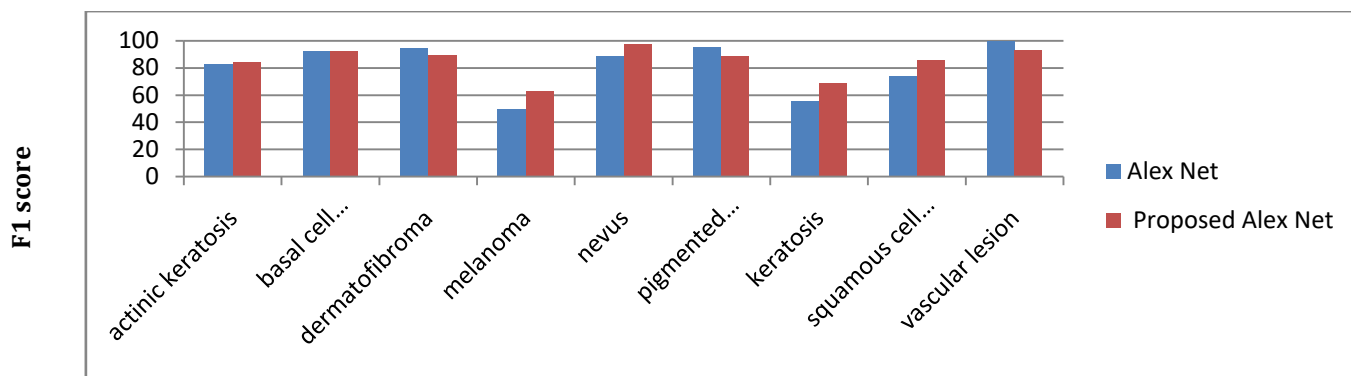


Figure 5: F1 scores comparison of Alex Net and Proposed Alex Net

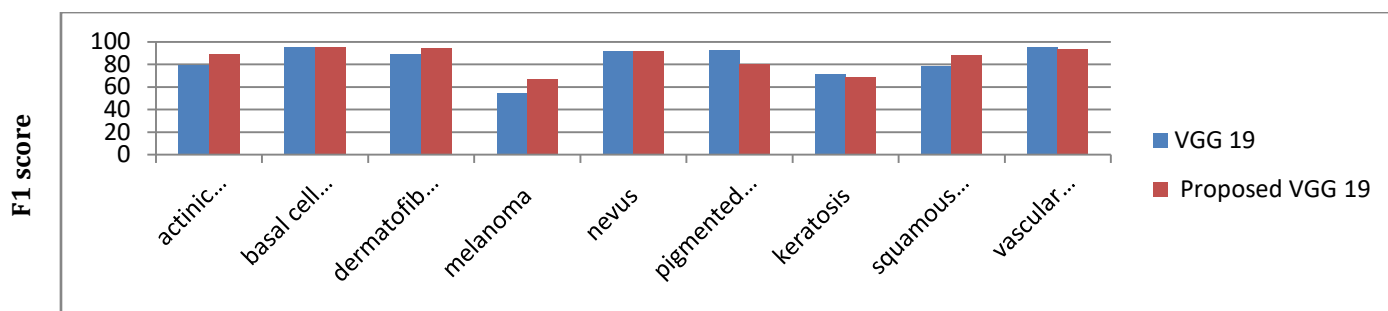


Figure 6: F1 scores comparison of VGG 19 and Proposed VGG 19

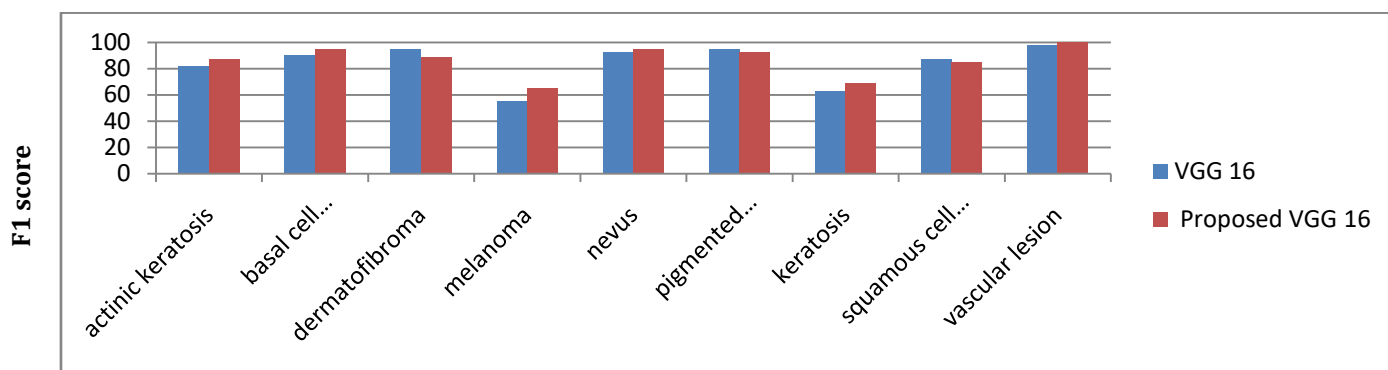


Figure 7: F1 scores comparison of VGG 16 and Proposed VGG 16

Figure 7 represents the F1 scores of VGG 16 and Proposed VGG 16. Out of Nine classes six classes improves their F1 score actinic keratosis, basal cell carcinoma, melanoma, nevus, keratosis, vascular lesion. Remaining are dermatofibroma, pigmented benign keratosis, squamous cell carcinoma.

By comparing three different networks the misclassification classes in Proposed Alex Net are improved in another network. F1 score of vascular lesion is improved in Proposed VGG 16, dermatofibroma F1 score is improved in Proposed VGG 19. Based on this concluded as each and every individual network extracted features in their own way so if we are able to fuse the features extracted from the proposed

networks overall classes F1 score will be improved.

4. CONCLUSION AND FUTURE SCOPE

In this investigation, a proposed model is presented that achieves a higher level of classification accuracy for skin cancer lesions. The model achieves this by combining features from various convolutional neural network (CNN) layers. Here tested proposed approach using the Skin Cancer ISIC dataset. Different CNN models, including AlexNet, VGG-19, and VGG-16, were evaluated to assess their individual classification performance. Among these models, VGG-16 demonstrated higher classification results on its own. Additionally, in this work introduced a fusion, suggesting that further improvement in

classification accuracy can be achieved by fusing the concepts of multiple networks. Based on these findings, in future plan to explore the fusion of multi-network concepts to enhance the classification accuracy even further. By

combining the strengths and features of different networks aim to improve the overall performance of the model and provide more accurate categorization of skin cancer lesions.

REFERENCES

1. American Cancer Society: Cancer facts and figures 2018. Available: <https://www.cancer.org/content/dam/cancer-org/research/cancer-factsand-statistics/annual-cancer-facts-and-figures/2018/cancer-facts-and-figures-2018.pdf>.
2. N. C. F. Codella et al., "Deep learning ensembles for melanoma recognition in dermoscopy images" IBM Journal of Research and Development, Vol.61, pp.5:1- 5:15, 2017.
3. Md. Shahin Ali, Md. SiponMiah, JahurulHaque,
4. Md. MahbuburRahman, Md. Khairul Islam. "An enhanced technique of skin cancer classification using deep convolutional neural network with transfer learning models", Machine Learning with Applications, 2021.
5. N. K. Mishra and M. E. Celebi. "An overview of melanoma detection in dermoscopy images using image processing and machine learning", 2016. Available: <https://arxiv.org/abs/1601.07843> , Accessed: 15 Aug 2018.
6. S. Thirumaladevi, K. VeeraSwamy and M. Sailaja, "Remote sensing image scene classification by transfer learning to augment the accuracy," Measurement: Sensors vol.25, pp.1-9, Jan. 2023.
7. Gutman, D. et al. Skin lesion analysis toward melanoma detection. International Symposium on Biomedical Imaging (ISBI),(International Skin Imaging Collaboration , 2016.
8. Binder, M. et al. Epiluminescence microscopy-based classification of pigmented skin lesions using computerized image analysis and an artificial neural network. *Melanoma Res.*, Vol. 8, pp. 261-266, 1998.
9. B.Petrovska, E. Zdravevski, P.Lameski, R.Corizzo, I. Stajduhar, and J. Lerga, "Deep learning for feature extraction in remote sensing: A case-study of aerial scene classification." *Sensors* vol. 20, no. 14, pp. 3906, 2020.
10. Burrioni, M. et al. Melanoma computer-aided diagnosis: reliability and feasibility study. *Clin. Cancer Res.*, Vol. 10, pp. 1881-1886, 2004.
11. S. Thirumaladevi, K. VeeraSwamy and M. Sailaja, "Improved transfer learning of CNN through fine-tuning and classifier ensemble for scene classification," *Soft Computing* vol.26, pp.5617-5636, April. 2022.
12. Schindewolf, T. et al. Classification of melanocytic lesions with color and texture analysis using digital image processing. *Anal. Quant. Cytol. Histol.*, Vol. 15, pp. 1-11, 1993.
13. Mnih, V. et al. Human-level control through deep reinforcement learning. *Nature*, vol. 518, pp. 529-533, 2015.